

# Detection of Multiple Influential Observations on Model Selection

Dongliang Zhang<sup>1</sup>    Masoud Asgharian<sup>2</sup>    Martin A. Lindquist<sup>1</sup>

<sup>1</sup>Department of Biostatistics, Johns Hopkins University, Baltimore, Maryland, U.S.A.

<sup>2</sup>Department of Mathematics and Statistics, McGill University, Montréal, Québec, Canada

## Abstract

Outlying observations are frequently encountered in a wide spectrum of scientific domains, posing significant challenges for the generalizability of statistical models and the reproducibility of downstream analysis. These observations can be identified through influential diagnosis, which refers to the detection of observations that are unduly influential on diverse facets of statistical inference. To date, methods for identifying observations influencing the choice of a stochastically selected sub-model have been underdeveloped, especially in the high-dimensional setting where the number of predictors  $p$  exceeds the sample size  $n$ . Recently we proposed an improved diagnostic measure to handle this setting. However, its distributional properties and approximations have not yet been explored. To address this shortcoming, the notion of exchangeability is revived, and used to determine the exact finite- and large-sample distributions of our assessment metric. This forms the foundation for the introduction of both parametric and non-parametric approaches for its approximation and the establishment of thresholds for diagnosis. The resulting framework is extended to logistic regression models, followed by a simulation study conducted to assess the performance of various detection procedures. Finally the framework is applied to data from an fMRI study of thermal pain, with the goal of identifying outlying subjects that could distort the formulation of statistical models using functional brain activity in predicting physical pain ratings. Both linear and logistic regression models are used to demonstrate the benefits of detection and compare the performances of different detection procedures. In particular, two additional influential observations are identified, which are not discovered by previous studies.

**Keywords:** clustering analysis; fMRI; high-dimensional diagnosis; influential point detection; logistic regression models; variable selection

# Contents

<b>1</b>	<b>Introduction</b>	<b>3</b>
<b>2</b>	<b>Methodology</b>	<b>4</b>
2.1	Review of Existing Literature . . . . .	4
2.2	Revival of Exchangeability . . . . .	5
2.3	Approximation via Parametric Approaches . . . . .	7
2.3.1	Thresholds for Diagnosis . . . . .	8
2.4	Approximation via Non-parametric Approaches . . . . .	9
2.4.1	Estimation Target . . . . .	9
2.4.2	Bootstrap Methods . . . . .	9
2.5	Detection of Multiple Influential Observations . . . . .	10
<b>3</b>	<b>Simulation Study</b>	<b>10</b>
3.1	Data Generation . . . . .	10
3.2	Method, Implementation and Assessment Metrics . . . . .	11
3.3	Simulation Results: Linear Regression Model . . . . .	11
3.4	Simulation Results: Logistic Regression Model . . . . .	12
<b>4</b>	<b>Pain Prediction using fMRI Data</b>	<b>13</b>
<b>5</b>	<b>Conclusions</b>	<b>15</b>

# 1 Introduction

In the era of “Big Data”, technological advancements have empowered unprecedented capability to produce, maintain, and analyze massive datasets. Yet, their sheer volume and high (or ultra-high) dimensionality do not always naturally translate into the traits necessary for extracting accurate and reproducible inference. One key hindrance is the presence of data heterogeneity in the form of outlying measurements. Indeed, primarily driven by large inter-subject differences and the inherent noisy nature of the data, such phenomenon is frequently observed in task-based functional magnetic resonance imaging (tfMRI) research, where measured signals are multivariate timeseries data of blood oxygenation level dependent (BOLD) responses taken at different brain locations (voxels) and time points.

As an undesirable result, this issue poses concerns for the generalizability of subsequent statistical models based on these data types, undermining their predictability and robustness, and the reliability of downstream statistical analysis. For this reason, influential diagnosis involving the detection of the subset of the data with excessive influence on various aspects of an estimated model should be conducted to detect influential or contaminated observations.

In the low-dimensional setting where the number of predictors  $p$  is less than the sample size  $n$ , extensive work exists to assess influence on a deterministic submodel. Yet, in practice, the mathematical form of a submodel is usually decided in a data-driven manner. In fact, when  $p$  surpasses  $n$ , high-dimensional model selectors are commonly used to derive scientifically meaningful information, which include but are not limited to the LASSO [26], scaled LASSO [23], SCAD [8] and MCP [30].

To date, the identification of observations influencing the stochastic choice of the selected submodel has been inadequately investigated. To illustrate the issue, a synthetic example is shown in Figure 1 (see Web Appendix A for details), where we observe that in the presence of multiple influential observations, the empirical probability of selecting an incorrect submodel from the reduced dataset upon partial or erroneous removal of the true influential points is non-negligible, underscoring the necessity to detect all the influential observations.

To identify these observations, [32] proposed the high-dimensional influence measure (HIM) to quantify the impact of a single point on the marginal correlation between the response variable and predictors. It is extended by [33] to detect numerous outliers, leading to the multiple influential points (MIP) detection method. Also, [21] developed the difference in model selected by the LASSO (DF(LASSO)) measure directly assessing the variation in submodels selected by LASSO. From this work, [31] introduced and justified the central limit theorem (CLT) for the generalized difference in model selection (GDF) metric that is applicable to general model selectors. Consistent high-dimensional clustering technique was then integrated with the GDF metric, giving rise to the clustering-based MIP (ClusMIP) algorithm to detect multiple influential observations.

However, the works of [21] and [31] are limited in two ways. First, the distributional properties of the DF(LASSO) and GDF metrics remain unexplored. Second, there is a lack of principled proposals to accurately approximate their distributions. This manuscript, with particular emphasis on methodological development, intends to consolidate and augment the results of [31] by extending the work on four fronts. First, we determine that the DF(LASSO) and GDF measures follow the Conway-Maxwell-Binomial distribution [14] and mixtures of binomial random variables, respectively, in finite- and

large-samples as  $p \rightarrow \infty$ . This is determined using the concept of exchangeability, which comprises three ingredients: the preservation of exchangeability [2], the characterization of sums of arbitrarily dependent sequence of events by their unique exchangeable counterparts [10], and the de Finetti’s Representation Theorem [5]. Second, we propose both parametric and non-parametric approaches to derive thresholds based on the mid-quantiles for diagnosis purposes. Specifically, the parametric candidates include the Conway-Maxwell-Binomial, Conway-Maxwell-Poisson [4], beta-binomial [22], generalized Poisson [3], and mixtures of binomial and Poisson distributions. Moreover, the non-parametric scheme encompasses three bootstrap methods [11, 19] designed for discrete, correlated data. Third, these approximation alternatives are incorporated into the ClusMIP procedure leading to a revised version, which is then extended for logistic regression models, available in a newly developed R package `ClusMIP`<sup>1</sup>. Fourth, high-dimensional linear and logistic regression models are applied to both simulated and real data to offer insights into the behaviors of different detection procedures. To practitioners, these four areas of improvement enhance the detection toolbox developed by [31] to allow detection of an even wider range of influential points, depending on the choice of model selector and approximation method.

The article is organized as follows: the existing literature is surveyed in Section 2.1. [31] is then reviewed and improved in Section 2.2, followed by introducing the parametric and non-parametric approaches in Sections 2.3 and 2.4, respectively. Extension to detect multiple influential points for the logistic regression model is given in Section 2.5. Sections 3 and 4 include simulations and the outlier detection analysis of an fMRI dataset collected to predict physical pain [18]. Conclusions are given in Section 5.

**Notation.** Let  $Y \in \mathbb{R}$  be the response variable and  $x_j \in \mathbb{R}$ ,  $j = 1, \dots, p$ , be the predictors. Let  $\mathbf{Y} = (Y_1, \dots, Y_n)^\top \in \mathbb{R}^n$  be the response vector and  $\mathbf{X} = (\mathbf{X}_1, \dots, \mathbf{X}_n)^\top \in \mathbb{R}^{n \times p}$ , where  $\mathbf{X}_i = (X_{i1}, \dots, X_{ip})^\top \in \mathbb{R}^p$ ,  $i = 1, \dots, n$ , be the  $n \times p$  design matrix. Then, the  $i^{\text{th}}$  observation or point of full dataset  $\mathbf{Z} := (\mathbf{Y}, \mathbf{X})$  is  $Z_i := (Y_i, \mathbf{X}_i^\top)^\top \in \mathbb{R}^{p+1}$ ,  $i = 1, \dots, n$ . Moreover, we abbreviate an arbitrary sequence of random variables or real values  $a_1, \dots, a_n$  by  $a_{[n]}$ .

## 2 Methodology

### 2.1 Review of Existing Literature

**HIM.** For  $i = 1, \dots, n$ , consider the linear regression model with *i.i.d.* errors  $\sigma^2 > 0$ :

$$Y_i = \mathbf{X}_i^\top \boldsymbol{\beta} + \epsilon_i, \quad \epsilon_i \sim N(0, \sigma^2), \quad (1)$$

where  $\boldsymbol{\beta} = (\beta_1, \dots, \beta_p)^\top \in \mathbb{R}^p$  is the regression coefficient. Under (1), [32] proposed the high-dimensional influence measure (HIM) to evaluate the effect of an individual point on the marginal correlation between the response variable and all the predictors. Specifically, the sample marginal correlation with the  $i^{\text{th}}$  observation removed is  $\hat{\rho}_j^{(i)} = \frac{\sum_{k=1, k \neq i}^n \{(X_{kj} - \hat{\mu}_{xj}^{(i)})(Y_k - \hat{\mu}_y^{(i)})\}}{\{(n-1)\hat{\sigma}_{xj}^{(i)}\hat{\sigma}_y^{(i)}\}}$ , where  $\hat{\mu}_{xj}^{(i)} = \frac{\sum_{k=1, k \neq i}^n X_{kj}}{n}$ ,  $\hat{\mu}_y^{(i)} = \frac{\sum_{k=1, k \neq i}^n Y_k}{n}$ ,  $(\hat{\sigma}_{xj}^{(i)})^2 = \frac{\sum_{k=1, k \neq i}^n (X_{kj} - \hat{\mu}_{xj}^{(i)})^2}{(n-1)}$ , and  $(\hat{\sigma}_y^{(i)})^2 = \frac{\sum_{k=1, k \neq i}^n (Y_k - \hat{\mu}_y^{(i)})^2}{(n-1)}$ . Then, aggregating over all  $p$  predictors gives the HIM  $\mathcal{D}_i = \sum_{j=1}^p (\hat{\rho}_j^{(i)} -$

<sup>1</sup>Available to be downloaded from <https://github.com/Dongliang-JHU/ClusMIP>.

$\widehat{\rho}_j^{(i)2}/p$ ,  $i = 1, \dots, n$ , where  $\widehat{\rho}_j^{(i)}$  is given above and  $\widehat{\rho}_j$  is its counterpart computed from the full dataset. Under certain conditions [*ibid.*, Conditions C.1-C.3, Section 2.3], it is shown that  $n^2\mathcal{D}_i \rightarrow \chi^2(1)$  as  $\min(n, p) \rightarrow \infty$ , where  $\chi^2(1)$  is the chi-square distribution with one degree of freedom, serving as the basis to determine a threshold for diagnosis purposes.

**MIP.** [33] decomposed multiple outlier identification into the simpler task of detecting a single point by incorporating the random-group-deletion (RGD) scheme into the modified HIM framework. Specifically, for each  $Z_i$ ,  $i = 1, \dots, n$ , the RGD randomly draws  $m$  subsets  $A_1, \dots, A_m$  with equal size from the remaining portion and attaches each of them to  $Z_i$ , one at a time. If  $Z_i$  is indeed influential and  $m$  is sufficiently large, there is a high probability that  $Z_i$  is the sole contaminated point in the subset indexed by  $A_j \cup \{i\}$  for some  $1 \leq j \leq m$ . Then, for each  $Z_i$ , two thresholding statistics  $T_{\min, i, m}$  and  $T_{\max, i, m}$  are proposed, which are the minimum and maximum versions of the foregoing HIM computed over all  $m$  subsets. They are shown [*ibid.*, Theorem 1] to be  $\chi^2(1)$  asymptotically and able to overcome the so-called swamping and masking effects in identifying multiple influential points. Indeed, the approach is theoretically justified [*ibid.*, Theorem 4] to be both functionally effective and computationally efficient. We refer to Web Appendix B for details of the RGD scheme and the MIP algorithm. In practice, the MIP is coded in the R package MIP.

**DF(LASSO).** [21] proposed the difference in model selection via the LASSO (DF(LASSO)) benchmark to directly quantify the influence of each individual point on the submodel selected by LASSO. This is defined by  $\widetilde{\delta}_i = (\delta_i - \mathbb{E}(\delta_i)) / \sqrt{\text{Var}(\delta_i)}$ , where  $\delta_i = \sum_{j=1}^p |\mathbb{1}(\widehat{\beta}_{\text{LASSO}, j} = 0) - \mathbb{1}(\widehat{\beta}_{\text{LASSO}, j}^{(i)} = 0)|$  and  $\mathbb{1}(\cdot)$  is the indicator function. Here,  $\widehat{\beta}_{\text{LASSO}, j}$  and  $\widehat{\beta}_{\text{LASSO}, j}^{(i)}$  respectively denote the  $j^{\text{th}}$  component of the LASSO estimates obtained from the full and reduced dataset without the  $i^{\text{th}}$  observation. The CLT of  $\delta_i$  is then derived [*ibid.*, Proposition 1] so that any point  $i$  with  $|\widetilde{\delta}_i| \geq 2$  is deemed influential. In practice, the sample mean and variance of  $\delta_{[n]}$  are suggested to replace  $\mathbb{E}(\delta_i)$  and  $\text{Var}(\delta_i)$  in computing  $\widetilde{\delta}_i$ 's.

## 2.2 Revival of Exchangeability

[31] relaxed the restriction on model selectors used the in DF(LASSO) and introduced the following generalized difference in model selection (GDF) metric:

$$\tau_i = \sum_{j=1}^p |\mathbb{1}(\widehat{\beta}_j = 0) - \mathbb{1}(\widehat{\beta}_j^{(i)} = 0)|, \quad i = 1, \dots, n, \quad (2)$$

where  $\widehat{\beta}_j$  and  $\widehat{\beta}_j^{(i)}$  are the  $j^{\text{th}}$  components of coefficient estimates from a sparse regression computed from the full and reduced dataset without  $i^{\text{th}}$  observation, respectively. To approximate the distribution of  $\tau_i$ , the authors derive [*ibid.*, Theorem 2] the CLT for  $\tau_i$  as  $p \rightarrow \infty$  by characterizing  $\tau_i$  as the sum of  $p$  exchangeable binaries [10], followed by applying the CLT to an exchangeable sequence of random variables [16]. Moreover, the sample mean and variance of  $\tau_{[n]}$  are shown to reliably estimate  $\mathbb{E}(\tau_i)$  and  $\text{Var}(\tau_i)$  in adopting the CLT. This is achieved via showing  $\tau_{[n]}$  to be exchangeable [Theorem 1, [31]] from the preservation of exchangeability [2], and is further corroborated by the uniform consistency of the empirical cumulative distribution function and law of large numbers for an exchangeable sequence of random variables. Yet, [31] lacks (i) a systematic study on the distributional properties of  $\tau_i$ , and (ii) investigation on alternative approximations to the distribution of  $\tau_i$ .

To describe the distribution of  $\tau_i$ , we first note that  $\tau_i$  is identically distributed as  $\sum_{j=1}^p \xi_{ij}$ , where  $\xi_{[p]}$  (upon suppressing the subscript  $i$ ) is an exchangeable sequence of Bernoulli random variables [10]. Then, the dependence in  $\xi_{[p]}$  is given by the lemma below, which is useful for parametric modeling discussed later. Its proof is provided in Web Appendix C.

**Lemma 1.** *Let  $\xi_{[p]}$  be the sequence of exchangeable Bernoulli summands for each  $\tau_i$  in (2) as discussed above. Then  $\text{Cov}(\xi_{iw}, \xi_{il}) \geq -\frac{\sigma^2}{p-1}$  for  $w \neq l$ , where  $\text{Var}(\xi_{ij}) = \sigma^2$ .*

Moreover, the de Finetti's Representation Theorem [5] (dFRT) indicates that as  $p \rightarrow \infty$ ,  $\xi_{[p]}$  is *i.i.d.*, conditional on the random variable  $\Theta$  associated with the probability measure  $\mu_\infty$ , where  $\Theta$  is the limiting relative frequency of confirming instances and  $\mu_\infty$  is the limiting distribution function of the empirical measure. This implies that asymptotically,  $\xi_{[p]}$  is unconditionally a mixture of an infinite *i.i.d.* Bernoulli sequence. Therefore, each  $\tau_i$  is the sum of a mixture of *i.i.d.* binaries as  $p \rightarrow \infty$ . Since summing *i.i.d.* Bernoulli random variables leads to a binomial random variable, the asymptotic distributions of  $\tau_i$  ((2)) is stated in the theorem below, whose proof is provided in Web Appendix D:

**Theorem 2.** *Let  $\tau_i$  be the GDF metric in (2). Then  $\tau_i$  is distributed according to a finite mixtures of binomial distributions as  $p \rightarrow \infty$ .*

Given that each  $\delta_i$ , the DF (LASSO) measure, is a special functional case of  $\tau_i$ , the following corollary is an immediate consequence of Theorem 2:

**Corollary 3.** *Let  $\delta_i$  be defined as in the DF(LASSO) approach (see Section 2.1),  $i = 1, \dots, n$ . Then each  $\delta_i$  is also a mixture of binomial random variables as  $p \rightarrow \infty$ .*

Having justified the large-sample distributions of  $\tau_i$  and  $\delta_i$ , we now characterize the distributional properties of the de Finetti mixing measure  $\mu_\infty$ . In fact, an exchangeable sampling scheme from an elementary Pólya urn model with two colored balls indicates that  $\mu_\infty$  is a beta distribution. However, if such sampling strategy is extended to a scheme with more than two colored balls,  $\mu_\infty$  is a Dirichlet distribution [17]. Indeed, this result is not a mere coincidence: [13] and [29] showed that for an exchangeable sequence of discrete random variables  $X_{[n]}$ , if the predictive probability  $\mathbb{P}(X_{n+1}|X_{[n]})$  has a specific linear form for any  $n$ , then  $\mu_\infty$  is indeed the Dirichlet distribution. In fact, such an assumption on the mathematical structure of  $\mathbb{P}(X_{n+1}|X_{[n]})$ , denoted Johnson's "sufficientness" postulate, has its philosophical origin traced back to the Laplace's Rule of Succession for enumerative induction. The foregoing discussion offers insight on characterizing the distributions of the de Finetti mixing measure  $\mu_\infty$ . We refer to [28] for a recent account.

On the other hand, we recognize that Theorem 2, Corollary 3 and the dFRT are asymptotically justified, failing to hold for the finite exchangeable sequence of binaries  $\xi_{[p]}$  [6]. Yet, the finite-sample variant of the dFRT [*ibid.*, Theorem 3] reveals that when  $p$  is large albeit finite, the distribution of the first  $k$  elements of  $\xi_{[p]}$  is in reasonable proximity to the de Finetti-type representation. This suggests that the binomials mixtures can be considered a proper approximation to the finite-sample distribution of  $\tau_i$  in (2).

In summary, we have (i)  $\tau_{[n]}$  is marginally identically distributed, (ii) in finite samples, each  $\tau_i$  is identically distributed as the sum of  $p$  exchangeable Bernoulli random variables with non-negative pairwise covariance as  $p \rightarrow \infty$  (Lemma 1), and (iii) each  $\tau_i$  or  $\delta_i$  is distributed as a mixture of binomials as  $p \rightarrow \infty$  (Theorem 2 and Corollary 3). They form the foundation for alternative approximations to  $\tau_i$  or  $\delta_i$ , which we present in Sections 2.3 and 2.4.

## 2.3 Approximation via Parametric Approaches

We note that the  $\tau_{[n]}$  are not independent. Yet, given that the sequence is exchangeable,  $\tau_i$ 's are identically distributed. Let  $F_\tau$  denote the true common distribution of  $\tau_i$ . To parametrically approximate  $F_\tau$ , we must first study the legitimacy of the maximum likelihood estimation (MLE) principle for parameter estimation. Under general regularity conditions, Theorem 4 validates the point estimation consistency of the minimizer of the Kullback-Leibler (K-L) divergence between  $F_\tau$  and the postulated family of parametric distributions. These regularity conditions and the proof of the theorem are given in Web Appendix E.

**Theorem 4.** *Let  $G_\theta$  be a parametric distribution indexed by the  $q$ -dimensional parameter  $\theta \in \Theta \subseteq \mathbb{R}^q$ , where  $\Theta$  is a bounded open set, and  $F_\tau$  be the true common distribution function of  $\tau_i$ 's. Suppose conditions (A.1) to (A.5) (see Web Appendix E) hold. Then  $\hat{\theta}_n \xrightarrow{p} \theta^*$  as  $n \rightarrow \infty$ , where  $\hat{\theta}_n$  is the MLE estimator obtained upon fitting  $G_\theta$  to  $\tau_{[n]}$  as if  $\tau_{[n]}$  was independent, and  $\theta^* = \operatorname{argmin}_{\theta \in \Theta} D_{KL}(\hat{F}_n || G_\theta)$ , the K-L divergence between  $\hat{F}_n$  and  $G_\theta$ .*

Founded on the exchangeability property of  $\tau_{[n]}$ , Theorem 4 advocates the MLE method although the independence of  $\tau_{[n]}$  fails to hold. Toward that end, we recognize that the MLE method is indeed asymptotically tantamount to minimizing the K-L divergence between  $\hat{F}_n$  and  $G_\theta$ ,  $I(\hat{F}_n, G_\theta) = E_{\hat{F}_n}(\log[d\hat{F}_n/dG_\theta])$ , where  $\hat{F}_n$  is the empirical distribution of  $\tau_{[n]}$ . Since  $\hat{F}_n \xrightarrow{\text{a.s.}} F_\tau$  as  $n \rightarrow \infty$  [1], the target  $\theta^*$  is consistently estimated by  $\hat{\theta}_n$ , where  $G_{\theta^*}$  is the nearest element to  $F_\tau$  in terms of K-L divergence that can be achieved within the possibly misspecified family of parametric distributions  $G_\theta$ . In view of this theorem, we study six parametric proposals where the above conditions (A.1) to (A.5) are fulfilled:

**Conway-Maxwell-Binomial (CMB).** The CMB distribution ( $\text{CMB}(p, q, \nu)$ ) generalizes the binomial distribution in modeling the sum of  $p$  associated Bernoulli random variables. Specifically, while  $q$  is the success rate, the direction and degree of association is controlled by  $\nu$  where  $\nu > 1$  indicates negative association, and vice versa. Moreover, it is shown [Theorem 4, [14]] that a CMB random variable  $X \sim \text{CMB}(p, q, \nu)$  can be written as the sum of  $p$  exchangeable Bernoulli summands. By the uniqueness of the result of [10], the finite-sample distributions of  $\tau_i$  and  $\delta_i$  are stated in Theorem 5. Its proof is given in Web Appendix F. In practice, the CMB is coded in the R package `COMMULTREG`.

**Theorem 5.** *Let  $\tau_i$  be the GDF metric defined in (2) and  $\delta_i$  be the DF(LASSO) measure. Then, both of them are Conway-Maxwell-Binomial random variables in finite sample.*

**Conway-Maxwell-Poisson (CMP).** The CMP distribution [4] ( $\text{CMP}(\lambda, \nu')$ ) generalizes the Poisson distribution, where  $\lambda$  is the mean occurrence rate and  $\nu'$  is the scale of dispersion. It is advantageous in approximating  $\tau_i$  for two reasons. First, the formulation  $\tau_i$  advocates its modeling via the Poisson-type distribution. Indeed,  $\tau_{[n]}$  is a non-negative, discrete sequence of counts assessing discrepancies in selected submodels. Moreover, Theorems 2 and 5 explicitly indicate that the binomial-type distribution characterizes the distribution of  $\tau_i$ . Second, dispersion does exist in  $\tau_{[n]}$ . By the preceding theorems,  $\tau_i$  follows a mixture distribution so that discrepancy in the mean and variance across subpopulations is possible, leading to dispersion in the data. Indeed, an observation biasing the choice of one predictor may well affect the selection of others. Such

positive association, shown by Lemma 1, contributes to over-dispersion in the dataset that is seen in Figure 2 (see Web Appendix G). In practice, the CMP distribution is coded in the R package `ComPoissonReg`.

**Beta-binomial (BB) and Generalized Poisson (GP).** The BB distribution ( $\text{BB}(\alpha, \beta)$ ) is another candidate to model association among the Bernoulli summands for  $\tau_i$  and is available in the R package `iZID`. Moreover, the GP distribution ( $\text{GP}(\theta, \lambda')$ ) captures the dispersion in  $\tau_i$ 's via the parameter  $\lambda'$ . Indeed, a GP random variable is identically distributed as a Poisson mixture [Theorem 2.1, [12]], approximating a binomial mixture, the asymptotic distribution of  $\tau_i$  (Theorem 2). It is coded in the R package `VGAM`.

**Mixtures of Binomial (MB) and Poisson (MP).** To directly model  $\tau_i$  by finite mixtures supported by Theorem 2, it is necessary to account for the identifiability of finite mixtures. Indeed, [25] established that the binomial mixtures are identifiable if and only if  $n \geq 2K - 1$ , where  $K$  is the order of finite mixtures. In this case,  $K$  is selected by the singular BIC criterion [7], developed to handle the singularity in the Fisher information matrix of the finite mixture models, which is implemented in the R package `sBIC`. In comparison, serving as approximations to binomial mixtures, Poisson mixtures are always identifiable [9] where the order is chosen by a sequential procedure based on the likelihood ratio test [15]. Parameters of the binomial and Poisson mixtures can be subsequently estimated via the Expectation-Maximization algorithm.

### 2.3.1 Thresholds for Diagnosis

Due to the discreteness of  $\tau_{[n]}$ , the sample quantile of the parametric approximating distribution in estimating its true counterpart may not be consistent. Toward that end, for detection purposes, a variant of quantile, called mid-quantile, is shown to exhibit promising asymptotic property. Specifically, let  $F_\tau$  be the true CDF of the random variable  $\tau$  with probability mass function  $p_\tau(x) = \mathbb{P}(\tau = x)$ , where  $\tau$  is supported on  $\{1, \dots, p\}$ . Then, for  $\zeta \in (0, 1)$ , the  $(100 \times \zeta)^{\text{th}}$  population mid-quantile  $Q_{\zeta, \text{mid}}$  is

$$Q_{\zeta, \text{mid}} = \begin{cases} 1, & \text{if } \zeta < F_{\text{mid}}(1), \\ k, & \text{if } \zeta = F_{\text{mid}}(k), \ k = 1, \dots, p, \\ \lambda k + (1 - \lambda)(k + 1), & \text{if } \zeta = \lambda F_{\text{mid}}(k) + (1 - \lambda)F_{\text{mid}}(k + 1), \ \lambda \in (0, 1), \\ p, & \text{if } \zeta > F_{\text{mid}}(p), \end{cases} \quad (3)$$

where  $F_{\text{mid}}(\cdot)$ , called the mid-distribution function, is given by  $F_{\text{mid}}(x) = F_\tau(x) - 0.5p_\tau(x)$ . Based on (3), for a given candidate  $G_\theta$ , the empirical and parametric approximating counterparts of  $Q_{\zeta, \text{mid}}$ , denoted by  $\tilde{Q}_{\zeta, \text{mid}}$  and  $\hat{Q}_{\zeta, \text{mid}, G_\theta}$ , are obtained by replacing the  $F_{\text{mid}}(\cdot)$  in (3) by  $\tilde{F}_{\text{mid}}(\cdot)$  and  $\hat{F}_{\text{mid}, G_\theta}(\cdot)$ , respectively. Here,  $\tilde{F}_{\text{mid}}(x) = \sum_{i=1}^n (\mathbb{1}(\tau_i \leq x) - 0.5\mathbb{1}(\tau_i = x))/n$ , and  $\hat{F}_{\text{mid}, G_\theta}(x) = G_\theta(X \leq x) - 0.5\mathbb{P}(X = x)$ , where  $X \sim G_\theta$ . It is then shown [*ibid.*, Theorem 2] that  $\sqrt{n}(\tilde{Q}_{\zeta, \text{mid}} - Q_{\zeta, \text{mid}})$  is asymptotically normal if  $\zeta$  does not correspond to  $F_{\text{mid}}(\cdot)$  evaluated at the boundary values 1 and  $p$ . As such, the empirical mid-quantile of  $\tau_{[n]}$ ,  $\tilde{Q}_{\zeta, \text{mid}}$ , is an appropriate candidate for the threshold. Yet, it falls short in practice since influential observations are always constrained to a given  $\tilde{Q}_{\zeta, \text{mid}}$ , which may not be realistic. In view of that, despite a lack of formal study on the convergence property of  $\sqrt{n}(\hat{Q}_{\zeta, \text{mid}, G_\theta} - Q_{\zeta, \text{mid}})$ , we observe that  $\sqrt{n}(\hat{Q}_{\zeta, \text{mid}, G_\theta} - Q_{\zeta, \text{mid}}) = \sqrt{n}(\hat{Q}_{\zeta, \text{mid}, G_\theta} - \tilde{Q}_{\zeta, \text{mid}}) + \sqrt{n}(\tilde{Q}_{\zeta, \text{mid}, G_\theta} - Q_{\zeta, \text{mid}})$ . While the second component vanishes asymptotically as mentioned above, the former is well controlled since  $\hat{Q}_{\zeta, \text{mid}, G_\theta}$  is obtained by fitting  $G_\theta$  to  $\tau_{[n]}$ . Therefore, assigning  $\hat{Q}_{\zeta, \text{mid}, G_\theta}$  for a given  $G_\theta$  as the threshold would be a reasonable alternative.



## 2.4 Approximation via Non-parametric Approaches

We now present three bootstrap schemes to derive appropriate thresholds for  $\tau_{[n]}$ .

### 2.4.1 Estimation Target

The estimation target is a cut-off point for diagnosis purposes. Its selection governs the formation of the statistical functional  $T_n = T_n(\tau_{[n]})$ , where functional differentiability is vital to justify the consistency of the bootstrap estimators. Toward that end, we consider three quantities of interest based on  $\tau_{[n]}$  with justified bootstrap approaches.

1. **Mean:**  $\mu = E(\tau_i)$ , estimated by  $T_n = T_n(\tau_1, \dots, \tau_n) = \sum_{i=1}^n \tau_i/n$  and interpreted as the average influence of an observation on variable selection. The upper bound of the associated bootstrap confidence interval serves as a reasonable threshold for diagnosis purposes.
2. **Quantile and mid-quantile:** given  $\zeta \in (0, 1)$ , the quantile  $Q_\zeta$  is defined by  $Q_\zeta = \inf_t \{t : F(t) \geq \zeta\}$  where  $F(\cdot)$  is the CDF and the mid-quantile  $Q_{\zeta, \text{mid}}$  is defined in (3). As explained below, their sample versions obtained via the bootstrap scheme [11] exhibit favorable large-sample properties, serving as reasonable threshold candidates.

### 2.4.2 Bootstrap Methods

With the three targets, we now present three bootstrap schemes.

**Method I.** [19] studied the legitimacy of directly bootstrapping an exchangeable sequence of random variables  $W_{[n]}$  when the statistical functional  $T_n$  has a linear form  $T_n = T_n(W_1, \dots, W_n) = \sum_{i=1}^n f(W_i)/n$ , where  $f : \mathbb{R} \rightarrow \mathbb{R}$  is a Borel-measurable function. Specifically, by the dFRT and its relevant extension, there exists a random variable  $\Lambda$  conditioning on which  $W_{[n]}$  is *i.i.d.* and belongs to the exponential family. Moreover,  $\Lambda$  is the limiting distribution of  $T_n$ . Then, upon randomly and uniformly drawing  $W_1^*, \dots, W_n^*$  with replacement from the original data, [19] showed [*ibid.*, Theorem 3.4] that the empirical distribution of  $T_n^* = T_n(W_1^*, \dots, W_n^*)$  reasonably approximates the distribution of  $T_n(W_1^*, \dots, W_n^* | W_1, \dots, W_n)$ , which in turn mimics the conditional distribution of  $\Lambda | W_1, \dots, W_n$ . In other words, the limiting conditional distribution of  $\Lambda$  is in close vicinity to the empirical distribution of the bootstrap estimator. Indeed, the authors established [*ibid.*, Theorem 3.7] that under regularity conditions,  $(\sqrt{n}(T_n^* - T_n)/S_n - \sqrt{n}(T_n - \Lambda)/S_n) | W_1, \dots, W_n \rightarrow 0$ , where  $S_n^2 = \sum_{i=1}^n (f(W_i) - T_n)^2/n$ . In our case,  $\tau_{[n]}$  plays the role of  $W_{[n]}$  in the preceding analysis and  $f$  is the identity function. The conditional distribution of  $\Gamma | \tau_1, \dots, \tau_n$  is then well approximated by empirical distribution of the bootstrap samples  $T_n^* = T_n(\tau_1^*, \dots, \tau_n^*) = \sum_{i=1}^n \tau_i^*/n$ , where  $\Gamma$  is the limiting distribution of  $T_n = T_n(\tau_1, \dots, \tau_n) = \sum_{i=1}^n \tau_i/n$ . Therefore, a feasible choice of the threshold would be the upper bound of the bootstrap confidence interval of  $T_n^*$ .

**Methods II and III.** Under the *i.i.d.* or strictly stationary settings, [11] proposed two *m*-out-of-*n* bootstrap schemes to directly re-sample the original, discrete data so that the distributions of its sample mid-quantile  $\tilde{Q}_{\zeta, \text{mid}}$  (3) and sample quantile  $\tilde{Q}_\zeta$  can be consistently approximated by their analogues of the bootstrap samples. Specifically, the *m*-out-of-*n* bootstrap involves randomly and uniformly drawing a sample of size *m* with replacement from the original data. Suppose  $m/n + 1/m = o(1)$ , the Kolmogorov-Smirnov (KS) distance between  $\tilde{Q}_{\zeta, m}^*$  and  $\tilde{Q}_\zeta$  is shown [*ibid.*, Theorem 8] to vanish as  $n \rightarrow \infty$ , where

$\tilde{Q}_{\zeta,m}^*$  is the sample quantile of the bootstrap samples from the  $m$ -out-of- $n$  bootstrap. Also, the KS distance between  $\sqrt{m}(\tilde{Q}_{\zeta,\text{mid},m}^* - \tilde{Q}_{\zeta,\text{mid}})$  and  $\sqrt{n}(\tilde{Q}_{\zeta,\text{mid}} - Q_{\zeta,\text{mid}})$  also converges to zero [*ibid.*, Corollary 18], where  $\tilde{Q}_{\zeta,\text{mid},m}^*$  and  $Q_{\zeta,\text{mid}}$  are the bootstrap and the true mid-quantiles, respectively. Therefore, applying these two bootstrap schemes directly to  $\tau_{[n]}$  obtains reliable sample quantiles and mid-quantiles from the bootstrap samples for diagnosis purposes.

## 2.5 Detection of Multiple Influential Observations

[31] proposed the ClusMIP method to detect multiple outliers. Specifically, the data is first divided into two components denoting the potentially influential ( $\hat{S}_{\text{infl}}$ ) and clean ( $\hat{S}_{\text{clean}}$ ) portions via a consistent high-dimensional clustering scheme. Candidates for such a procedure include, but are not limited to spectral clustering [20] and regularized  $K$ -means clustering [24]. Then, each  $i \in \hat{S}_{\text{infl}}$  is studied by considering the combined dataset indexed by  $\{i\} \cup \hat{S}_{\text{clean}}$ . If it is truly influential, asymptotically it would be the sole influential observation in the merged subset, an argument supported by the strong consistency of the clustering procedure. Thus, the scheme to detect a single influential point can then be administered, consisting of the CLT [31] and the newly proposed parametric and non-parametric approaches. This expands the approximation toolbox of the original ClusMIP procedure, leading to its revised version provided in Web Appendix H.

Now, consider the logistic regression model given by

$$\log(\mathbb{P}(Y_i = 1)/(1 - \mathbb{P}(Y_i = 1))) = \mathbf{X}_i^\top \boldsymbol{\phi}, \quad Y_i \in \{0, 1\}, \quad i = 1, \dots, n, \quad (4)$$

where  $\boldsymbol{\phi} = (\phi_1, \dots, \phi_p)^\top \in \mathbb{R}^p$  is the regression coefficient. To detect multiple influential points under (4), we analogously perform data partition followed by refined assessment. In contrast to (1), the generation mechanism under (4) necessitates different clustering techniques based on the contamination types. Toward that end, the Expectation-Maximization algorithm could be a suitable option when the heterogeneity originates from the finite mixture of logistic regressions. However, in practice, we recognize that the resulting clustering is sensitive to the starting points, considerably mitigating the efficacy of the subsequent examination. Thus, in our following simulation, we only consider the simple case of admitting contamination solely to the predictors, where the foregoing clustering choices are effective. Both (1) and (4) are implemented in an R package `ClusMIP` available from the first author's GitHub page.

## 3 Simulation Study

We now perform a simulated study to examine the performances of the two existing proposals and the newly proposed revised ClusMIP detection procedure.

### 3.1 Data Generation

**Design Matrix  $\mathbf{X}$ .** The design matrix  $\mathbf{X} = \mathbf{X}(\Sigma(\rho))$  follows a multivariate normal distribution with mean  $\mathbf{0}$  and covariance matrix  $\Sigma(\rho)$ , where the  $(i, j)$ -entry is given by  $\Sigma_{i,j}(\rho) = \rho^{|i-j|}$  and  $\rho \in \{0, 0.5\}$ . Moreover,  $(n, p)$  are set to be  $(50, 200)$  under (1) and  $(100, 200)$  under (4).

**Influential and Clean Observations.** Given the design matrix  $\mathbf{X}(\Sigma(\rho))$  and regression coefficients, the responses  $Y_i, i = 1, \dots, n$ , are first homogeneously generated by the linear (1) or logistic regression model (4). Then, the first  $n_{\text{infl}} = 10$  observations are replaced by their contaminated counterparts produced by the perturbation models discussed below. This leads to the contaminated dataset containing  $n_{\text{infl}}$  influential and  $n - n_{\text{infl}}$  clean observations.

**Perturbation Models.** Under (1), we consider three perturbation models. The first is obtained by adding contamination controlled via the parameter  $\kappa_{\text{linear}, \mathbf{Y}} \in \{5, 10, 30\}$  to the response vector, while the predictors is unchanged. The second is formulated by incorporating contamination controlled by the parameter  $\kappa_{\text{linear}, \mathbf{X}} \in \{5, 10, 30\}$  into the first 10 predictors, while the response vector is intact. The third one is obtained by simultaneously including contamination dictated by the parameter  $\kappa_{\text{linear}, \mathbf{XY}} \in \{5, 10, 30\}$  to the response vector and the first 10 predictors. In comparison, under (4) and in view of the discussion at the end of Section 2.5, only the perturbation model contaminating the first 10 predictors via  $\kappa_{\text{logistic}, \mathbf{X}} \in \{5, 10, 30\}$  is studied. The perturbation model details are given in Web Appendix I.

### 3.2 Method, Implementation and Assessment Metrics

Based on (1), the revised ClusMIP is applied to the LASSO, scaled LASSO (SLASSO), SCAD and MCP as model selectors. Specifically, it includes ten second-stage approximations to the distribution of  $\tau_i$ , the CLT [31], six parametric approximating approaches (Param-CMB, Param-CMP, Param-BB, Param-GP, Param-MB and Param-MP), and three bootstrap schemes (Boot-I, Boot-II and Boot-III). In the sequel, the abbreviation of the above approximating techniques is written as ClusMIP(Selector), where Selector represents the model selector. Moreover, the two existing proposals, DF(LASSO) and MIP methods, are also included. On the other hand, based on (4), the same revised ClusMIP procedure is applied to the LASSO, SCAD and MCP. Furthermore, while the DF(LASSO) is included, MIP is omitted as it is not designed for (4). In addition, the tuning parameter for all the regularized regressions are chosen via 10-fold cross-validation (CV). The method and implementation are summarized in Web Tables 1 and 2. For comparison purposes, two metrics are considered: the power (Power(Detection)) and the false positive rate (FPR(Detection)) of detection, where ‘‘Detection’’ is the detection procedure. They are formally defined in Web Appendix J.

### 3.3 Simulation Results: Linear Regression Model

The simulation results for  $\mathbf{X}(\Sigma(0.5))$  are schematically illustrated in Figure 3 while those for  $\mathbf{X}(\Sigma(0))$  demonstrate similar pattern and are reported in Web Appendix Figure 1. Moreover, the simulation results under Perturbation Model III are similar to those under Perturbation Model I and its analyses are provided in Web Appendix K.

#### **Perturbation Model I (Upper Panel of Figure 3):**

1. Power(DF(LASSO)) stays below 0.10 regardless of  $\kappa_{\text{linear}, \mathbf{Y}}$  due to its leave-one-out formulation. In contrast, as  $\kappa_{\text{linear}, \mathbf{Y}}$  rises from 5 to 10 and 20, Power(MIP) rises from 0.05 to 0.82 and 1.00. This implies that the MIP method may not capture influence on variable selection under the low perturbation magnitude, yet it performs well as the contamination intensifies.
2. While distinctive patterns are seen for the ClusMIP methods, all their detection

powers are above 0.40, surpassing those of MIP when  $\kappa_{\text{linear},\mathbf{Y}} = 5$ . Moreover, the detection power of ClusMIP(SLASSO) is consistently above 0.95 across all approximating approaches. Specifically, it reaches 1.00 as  $\kappa_{\text{linear},\mathbf{Y}}$  increases from 5 to 20. One exception is that slight variation is seen for the Param-BB approximation, where its detection power rises from 0.90 to 0.95 and 1.00 as  $\kappa_{\text{linear},\mathbf{Y}}$  increases. Indeed, this phenomenon is common: under-performance is always seen for Param-BB among the ten approximating methods. On the other hand, we observe that ClusMIP(SLASSO) always outperforms its competing proposals with a detection power exceeding 0.95. This indicates that SLASSO is sensitive to the presence of influential points irrespective of types of the second-stage approximating approaches.

**3.** In comparison with ClusMIP(SLASSO), the ClusMIP method applied to the LASSO, SCAD and MCP have noticeably lower power of detection. Specifically,  $\text{Power}(\text{ClusMIP}(\text{LASSO}))$  ranges from 0.45 to 0.90, with the lowest and highest value respectively attained through Param-BB and Boot-I. In fact, the Boot-I and CLT always achieve the highest detection power among the ten approximation candidates, which holds for the ClusMIP of all model selectors under all perturbation schemes. On the other hand,  $\text{Power}(\text{ClusMIP}(\text{LASSO}))$  for the remaining approximations are analogous in scales, fluctuating between 0.60 and 0.80.

**4.** High degree of resemblance is seen in the detection powers of the ClusMIP applied to SCAD and MCP, which ranges between 0.35 and 0.95. In contrast to  $\text{Power}(\text{ClusMIP}(\text{LASSO}))$ , mild variation is seen in  $\text{Power}(\text{ClusMIP})$  of SCAD and MCP as  $\kappa_{\text{linear},\mathbf{Y}}$  increases.

**5.** The FPR for all the procedures under all perturbation models fall below the nominal level  $\alpha = 0.05$ , validating the FPR control assertion in Theorem 3 from [31].

**Perturbation Model II (Middle Panel of Figure 3):**

**1.** Under-performance is observed for both DF(LASSO) and MIP methods, the detection power falls below 0.05 and 0.30, respectively, as  $\kappa_{\text{linear},\mathbf{X}}$  increases. Therefore, under this scenario, MIP and DF(LASSO) are outperformed by the ClusMIP procedure.

**2.** ClusMIP(SLASSO) consistently exhibits satisfactory performance as its detection power is almost 1.00 regardless of approximation approach. In contrast, large variation (between 0.20 and 1.00) is seen in  $\text{Power}(\text{ClusMIP}(\text{LASSO}))$ . Particularly, as  $\kappa_{\text{linear},\mathbf{X}}$  increases, both CLT and Boot-I provide favorable detection power (about 1.00 and 0.85). Yet,  $\text{Power}(\text{ClusMIP}(\text{LASSO}))$  for the rest of approximations fluctuate between 0.20 and 0.60.

**3.** The detection power for ClusMIP(SCAD) and ClusMIP(MCP) closely resemble their respective counterparts under Perturbation Model I. We note that the detection power of the CLT approximation reach 1.00 as the contamination intensifies.

### 3.4 Simulation Results: Logistic Regression Model

The simulation results for  $\mathbf{X}(\Sigma(0))$  and  $\mathbf{X}(\Sigma(0.5))$  are reported in Figure 4.

Under  $\mathbf{X}(\Sigma(0))$ , DF(LASSO) shows inadequate detection power (always below 0.05) which aligns with the phenomenon in Figure 3. On the other hand, at  $\kappa_{\text{logistic},\mathbf{X}} = 5$ ,  $\text{Power}(\text{ClusMIP})$  of LASSO, SCAD and MCP are much lower than their counterparts under (1), ranging between 0.05 and 0.40, 0.07 and 0.45, and 0.07 and 0.40, respectively. CLT and Param-BB yield the lowest detection power, while the highest level is achieved by Boot-I, which agrees with what was seen under (1). Moreover, as the contamination exacerbates, drastic improvement in detection power is observed for all the ClusMIP

procedures. Notably,  $\text{Power}(\text{ClusMIP})$  for the SCAD and MCP reaches at least 0.92 under Boot-I at  $\kappa_{\text{logistic}, \mathbf{X}} = 30$ . In comparison,  $\text{Power}(\text{ClusMIP})$  for the LASSO has its maximum below 0.70. In general,  $\text{Power}(\text{ClusMIP})$  of SCAD and MCP is higher than that of the LASSO at medium and high perturbation scales. The pattern of detection power under  $\mathbf{X}(\Sigma(0.5))$  is similar to the one under  $\mathbf{X}(\Sigma(0))$ . On the other hand, the FPR of all the detection methods are below the nominal level  $\alpha = 0.05$ .

## 4 Pain Prediction using fMRI Data

We now illustrate our method on a dataset for assessing the effect of physical pain on the brain using fMRI. The primary goal is to detect and interpret outliers by various procedures, and examine their impact on downstream analysis including variable selection and prediction.

**Description.** The experiment consisted of repeated thermal stimulation at six temperatures (44.3, 45.3, 46.3, 47.3, 48.3 and 49.3 °C) to the left forearm of 33 participants. After each stimuli, the amount of self-reported pain was recorded on a 200-point scale. Values above and below 100 represent high and low pain ratings, respectively. Pain scores were treated as our outcome of interest. Technical specifics on the acquisition, preprocessing, and analysis of the fMRI data can be found in [18]. In short, within-subject functional activation maps associated with each stimuli were estimated. These voxel-wise maps quantify the localized brain activation that arises due to the applied stimulus. The maps were further averaged over the repeated trials at each of the six temperatures, leading to 6 maps per participant, and further spatially averaged across 489 distinct brain regions. This produces a design matrix with 489 predictors, corresponding to the average temperature-specific brain activity in a specific brain region for each of the 33 participants, and 198 pain score responses.

**Method.** The dataset is investigated using both high-dimensional linear (1) and logistic (4) regression models. Under (4), a binary response vector of the pain rating is obtained by assigning ratings below 100 to be 0 and those above 100 to be 1. This particular threshold corresponds to where the participants consider the stimuli to be painful. Moreover, under (1), the DF(LASSO) and MIP, and the revised ClusMIP procedure applied to the LASSO, SLASSO, SCAD and MCP are considered. On the other hand, under (4), only the DF(LASSO) and the revised ClusMIP applied to the LASSO, SCAD and MCP are included.

**Assessment.** In addition to tabulating the estimated influential observations denoted by  $\hat{I}_{\text{linear}}(\text{Detection})$  under (1) and  $\hat{I}_{\text{logistic}}(\text{Detection})$  under (4), we also compute the predictive metrics and contrast the selection of brain regions before and after the removing the identified influential observations. These results are diagrammatically provided in Figures 5 and 6.

**Results.** The estimated influential points are given in Web Tables 3 to 6. Below we provide summaries of the results.

**A. Detection under (1):** significant variation in detected influential points exists in all detection procedures. No influential observations are detected by MIP and ClusMIP(SLASSO) (except for Param-CMP, GP and MP, and Boot-I, all of which indeed barely detect any influential observations). This corresponds to the results seen in the simulation study, Figure 3, where both procedures exhibit similar detection performance in most settings. In contrast, considerably more influential points are identified by the

ClusMIP procedure applied to the LASSO, SCAD and MCP, where  $|\widehat{I}_{\text{linear}}(\text{ClusMIP}(\text{LASSO}))| > |\widehat{I}_{\text{linear}}(\text{ClusMIP}(\text{SCAD}))| \approx |\widehat{I}_{\text{linear}}(\text{ClusMIP}(\text{MCP}))|$ . On the other hand, within each ClusMIP procedure, Boot-I always detects the largest number of influential points. To be specific, it respectively identifies 76, 8, 53 and 59 influential points for ClusMIP applied to the LASSO, SLASSO, SCAD and MCP. In contrast, Param-BB achieves the smallest number of detected observations, which is 34, 0, 3 and 14 accordingly. This corresponds with our simulation results, where the Boot-I and Param-BB achieves the highest and lowest detection powers, respectively.

**B. Detection under (4):** in contrast to (1), substantially less influential points are detected using (4). Similar to the above conclusion under (1), Boot-I and Param-BB have the most and least detected points, consistent with Figure 4. Moreover, under (4), for each approximating approach,  $|\widehat{I}_{\text{linear}}(\text{ClusMIP}(\text{SCAD}))| \approx |\widehat{I}_{\text{linear}}(\text{ClusMIP}(\text{MCP}))| > |\widehat{I}_{\text{linear}}(\text{ClusMIP}(\text{LASSO}))|$ . This aligns with our simulation (see Figure 4), where ClusMIP applied to SCAD and MCP is shown to have higher detection power than that of ClusMIP(LASSO).

**C. Distribution:** under both (1) and (4), for each model selector of the ClusMIP procedure, we further compute the commonly detected influential observations among the ten approximating candidates, provided in Table 1. These common influential observations are highlighted in the plot of pain ratings at six temperatures shown in Panels (B) to (D) of Figure 5. Based on this plot, we observe that under both (1) and (4), influential points tend to be located at lower pain levels ( $< 100$ ) corresponding to lower temperatures (44.3, 45.3 and 46.3 °C). This is reasonable since low pain felt at warm temperatures is considered non-painful, which may be better explained by a different model than that obtained using data corresponding to higher pain at higher temperatures.

Table 1: Indices of Estimated Influential Observations for the Physical Pain Prediction Dataset. For the ClusMIP procedure, they are obtained via extracting the commonly identified influential points among the ten approximating approaches discussed in Sections 2.3 and 2.4.

Procedures	Common $\widehat{I}_{\text{linear}}$	Common $\widehat{I}_{\text{logistic}}$
DF(LASSO)	2,6,72,121,130,138,174,181	23,73
MIP	NA	-
(Revised) ClusMIP(LASSO)	7,13,14,43,45,50,51,52,55,56,57,58,82,87, 103,104,127,133,134,145,147,171,172,175	13,111,166
(Revised) ClusMIP(SLASSO)	NA	-
(Revised) ClusMIP(SCAD)	44,124,163,165	4,22,74,83,135,148,170,188
(Revised) ClusMIP(MCP)	14,15,19,20,56,57,87,115,145,146,176	3,15,73,157

**D. Prediction:** under both (1) and (4), we examine the prediction performance before and after removing the detected influential points from Table 1. Specifically, both the full and reduced dataset are randomly divided into the training and testing sets where the regression coefficients are obtained on the training set while the predictive metrics are calculated on the test set. Under (1), the predictive metric is the Pearson’s correlation between observed and predicted pain scores; under (4), the metric is the accuracy of the observed and predicted binary pain scores. These metrics are computed and averaged over 1000 sampling splitting as mentioned above, leading to the results in Panel (A) of Figure 5. From this plot, we find at least a 10% enhancement in the predictive performance is

achieved by omitting the identified influential points under both (1) and (4), highlighting the benefit of their identification.

**E. Variation in brain region selection:** under both (1) and (4), a discrepancy in the selected brain regions and the intensities of regression coefficients is noted before and after the removal of detected influential points  $\hat{I}_{\text{linear}}$  and  $\hat{I}_{\text{logistic}}$ . While such variation exists for all detection procedures, to illustrate we focus on ClusMIP(LASSO) with Boot-I shown in Figure 6. The maps associated with the reduced dataset show improved quality. This can be seen by the reduction of selected regions near the boundary of the brain, which are typically activated by excessive subject motion, while retaining the key regions known to be involved in pain processing pathways (e.g., somatosensory S1/S2, medial thalamus, Anterior Cingulate, and mid insular-opercular areas). These findings are consistent for both (1) and (4).

**F. Practical guidelines:** variation in the model-dependent detection of influential points is observed, necessitating guidance on which influential points to be considered. In practice, a toolbox of model selectors is chosen by practitioners *a priori* based on exploratory analysis and domain science knowledge. Within our framework there are ample options available to practitioners ranging from taking the intersection to the union of all the influential point sets. Particular choices can then be made based on the practitioners’ data and domain expertise, and how conservative they are in their decision-making. In this case, influential points that are detected by both (1) and (4) when modeling physical pains are deemed important. Specifically, under Boot-I, let  $\hat{I}_{\text{common}} := \hat{I}_{\text{linear}} \cap \hat{I}_{\text{logistic}}$ . Then, the intersection of  $\hat{I}_{\text{common}}$  (ClusMIP) for LASSO, SCAD and MCP is  $\{49, 55, 61, 169\}$ . In comparison with [31], two extra observations  $\{61, 169\}$  are identified, corresponding to temperatures of 44.3°C. This reinforces our previous analysis (third point) that outlying observations tend to be linked with lower temperatures where not all participants experience pain. Indeed, from a philosophical perspective toward data science, our proposal is deliberately formulated to objectively provide a full spectrum of possible influential points based on the belief that we consider ourselves to be statistical toolbox providers, instead of decision makers. In fact, such perspective aligns with the Fisherian and Tukey’s view on data analysis, asserting that we “offer guidance, not the answer” [27]. Moreover, from a theoretical angle, the distinct behavior of model selectors in the presence of influential points serves as opportunity to explore their sensitivity and robustness to outlyingness in terms of variable selection, which has not been systematically studied.

## 5 Conclusions

This article extends the work in [31] to address the issue of detecting influential observations on variable selection. Specifically, the large- and finite-sample distributions of the GDF measure (2) and the DF(LASSO) measure [21] have been determined in Theorems 2 and 5, respectively. Six parametric (supported via Theorem 4) and three bootstrap schemes are proposed to approximate the distribution of  $\tau_i$  (2) and subsequently derive the threshold for detection of outlying observations. In particular, the mid-quantile is identified as a suitable candidate for such a thresholding statistic, resolving the inconsistency posed by the quantile of a sequence of discrete random variables. Integrating these newly proposed approaches into the ClusMIP algorithm [31] leads to its revised version in detecting multiple influential observations.

These methodological contributions are verified by simulation studies under both the high-dimensional linear (1) and logistic (4) regression models, from which we obtain the following.

1. **MIP and DF(LASSO)**. Under-performance of the DF(LASSO) exists under all simulation scenarios due to its leave-one-out design. Moreover, MIP attains favorable detection except for the perturbation scheme that introduces contamination solely into the predictors.
2. **ClusMIP(SLASSO)**. Consistently satisfactory performance is obtained for the revised ClusMIP method when applied to SLASSO under all settings, which almost always detect all the influential points. Therefore, ClusMIP(SLASSO) is recommended for detection purposes.
3. **ClusMIP of LASSO, SCAD, MCP**. Their detection power are noticeably lower than those of ClusMIP(SLASSO) across all approximation approaches. Moreover, for the same second-step approximation approach, while the revised ClusMIP applied to the LASSO, SCAD and MCP exhibit similar performance under (1), the revised ClusMIP(SCAD) and ClusMIP(MCP) have higher detection power than that of the ClusMIP(LASSO) under (4).
4. **Approximation Proposals**. Among the ten approximations, under (1), the parametric proposal via the beta binomial distribution (Param-BB) attains the lowest detection power, while the highest is achieved by the CLT [31] and the first bootstrap scheme (Boot-I) [19]. In comparison, under (4), the CLT and the Param-BB are out-performed by all the others, whereas the highest detection power is again obtained by the Boot-I. As such, as a general diagnosis guideline, while the behavior of the CLT depends on the model, the Boot-I approximation is recommended and Param-BB shall be avoided.
5. **Asymptotic Requirement**. The asymptotic validity of the CLT and the parametric methods depends on diverging  $n$  and  $p$ , yet only  $n \rightarrow \infty$  is needed for the bootstrap schemes.

The existing methods and the revised ClusMIP are also used to analyze a real dataset studying the effect of physical pain on the brain using fMRI. Besides consistent detection performance as seen in the simulated studies, improved predictive power is obtained upon removing identified outliers under both (1) and (4). Variation in finite-sample detection behaviors for the revised ClusMIP applied to different model selectors is yet to be explored.

**Acknowledgments** Dongliang Zhang is partially supported by NIH grant R01MH129397 from the National Institute of Mental Health. Martin A. Lindquist is supported in part by NIH grant R01 EB026549 from the National Institute of Biomedical Imaging and Bioengineering and R01MH129397 from the National Institute of Mental Health. Masoud Asgharian is supported by the Natural Science and Engineering Research Council of Canada (NSERC RGPIN-2018-05618)

## References

- [1] K. B. Athreya and V. Roy. General Glivenko-Cantelli theorems. *Stat*, 5(1):306–311, 2016.
- [2] D. Commenges. Transformations which preserve exchangeability and application to permutation tests. *Journal of Nonparametric Statistics*, 15(2):171–185, 2003.



- [3] P. C. Consul and G. C. Jain. A generalization of the Poisson distribution. *Technometrics*, 15(4):791–799, 1973.
- [4] R. W. Conway and W. L. Maxwell. A queuing model with state dependent service rates. *Journal of Industrial Engineering*, 12(2):132 – 136, 1962.
- [5] B. de Finetti. Funzione caratteristica di un fenomeno aleatorio. In *Atti del Congresso Internazionale dei Matematici*, page 179–190, 1929.
- [6] P. Diaconis and D. Freedman. Finite exchangeable sequences. *Ann. Probab.*, 8(4): 745–764, 1980.
- [7] M. Drton and M. Plummer. A Bayesian information criterion for singular models. *Journal of the Royal Statistical Society: Series B (Methodological)*, 79(2):323–380, 2017.
- [8] J. Fan and R. Li. Variable selection via nonconcave penalized likelihood and its oracle properties. *Journal of the American Statistical Association*, 96(456):1348–1360, 2001.
- [9] W. Feller. On a general class of "contagious" distributions. *The Annals of Mathematical Statistics*, 14(4):389 – 400, 1943.
- [10] János Galambos. *The asymptotic theory of extreme order statistics*. Wiley, 1978.
- [11] C. Jentsch and A. Leucht. Bootstrapping sample quantiles of discrete data. *Annals of the Institute of Statistical Mathematics*, 68:491–539, 2016.
- [12] H. Joe and R. Zhu. Generalized Poisson distribution: the property of mixture of Poisson and comparison with negative binomial distribution. *Biom. J.*, 47(2):219–229, 2005.
- [13] W. E. Johnson. Probability: Deductive and inductive problems. *Mind*, 41(164): 409–423, 1932.
- [14] J. B. Kadane. Sums of possibly associated Bernoulli variables: The Conway-Maxwell-Binomial distribution. *Bayesian Analysis*, 11(2):403–420, 2016.
- [15] D. Karlis and E. Xekalaki. On testing for the number of components in a mixed Poisson model. *Annals of the Institute of Statistical Mathematics*, 51(1):149–162, 1999.
- [16] M. Klass and H. Teicher. The central limit theorem for exchangeable random variables without moments. *Annals of Probability*, 15(1):138–153, 1987.
- [17] J. Lin. On the Dirichlet Distribution. Master’s thesis, Queen’s University, 2016.
- [18] M. A. Lindquist, A. Krishnan, M. López-Solà, M. Jepma, C.-W. Woo, L. Koban, M. Roy, L. Y. Atlas, L. Schmidt, L. J. Chang, E. A. R. Losin, H. Eisenbarth, Y. K. Ashar, E. Delk, and T. D. Wager. Group-regularized individual prediction: theory and application to pain. *NeuroImage*, 145:274–287, 2017.
- [19] P. Muliere and P. Secchi. Exchangeability, predictive sufficiency and bayesian bootstrap. *Journal of the Italian Statistical Society*, 1(3):377–404, 1992.

- [20] A. Ng, M. Jordan, and Y. Weiss. On spectral clustering: Analysis and an algorithm. In *Advances in Neural Information Processing Systems*, volume 14, 2001.
- [21] B. Rajaratnam, S. Roberts, D. Sparks, and H. Yu. Influence diagnostics for high-dimensional Lasso regression. *J. Comput. Graph. Stat.*, 28(4):877–890, 2019.
- [22] J. G. Skellam. A probability distribution derived from the Binomial distribution by regarding the probability of success as variable between the sets of trials. *Journal of the Royal Statistical Society: Series B (Methodological)*, 10(2):257–261, 1948.
- [23] T. Sun and C.-H. Zhang. Scaled sparse linear regression. *Biometrika*, 99(4):879–898, 2012.
- [24] W. Sun, J. Wang, and Y. Fang. Regularized  $k$ -means clustering of high-dimensional data and its asymptotic consistency. *Electron. J. Stat.*, 6:148 – 167, 2012.
- [25] H. Teicher. Identifiability of finite mixtures. *Ann. Math. Stat.*, 34(4):1265–1269, 1963.
- [26] R. Tibshirani. Regression shrinkage and selection with the LASSO. *Journal of the Royal Statistical Society. Series B (Methodological)*, 58:267–288, 1996.
- [27] J. W. Tukey. The Future of Data Analysis. *Ann. Math. Stat.*, 33(1):1–67, 1962.
- [28] E.-J. Wagenmakers, S. Zabell, and Q. F. Gronau. J. B. S. Haldane’s rule of succession. *arXiv:2307.09489*, 2023.
- [29] S. L. Zabell. W. E. Johnson’s “sufficientness” postulate. *Ann. Stat.*, 10(4):1090–1099, 1982.
- [30] C-H. Zhang. Nearly unbiased variable selection under minimax concave penalty. *Ann. Stat.*, 38(2):894–942, 2010.
- [31] D. Zhang, M. Asgharian, and M. A. Lindquist. Assessing influential observations in pain prediction using fMRI data. *arXiv:2401.13208*, pages 1–21, 2023.
- [32] J. Zhao, C. Leng, L. Li, and H. Wang. High-dimensional influence measure. *Annals of Statistics*, 41(5):2639 – 2667, 2013.
- [33] J. Zhao, C. Liu, L. Niu, and C. Leng. Multiple influential point detection in high dimensional regression spaces. *J. R. Stat. Soc. Ser. B Stat. Method.*, 81(2):385–408, 2019.

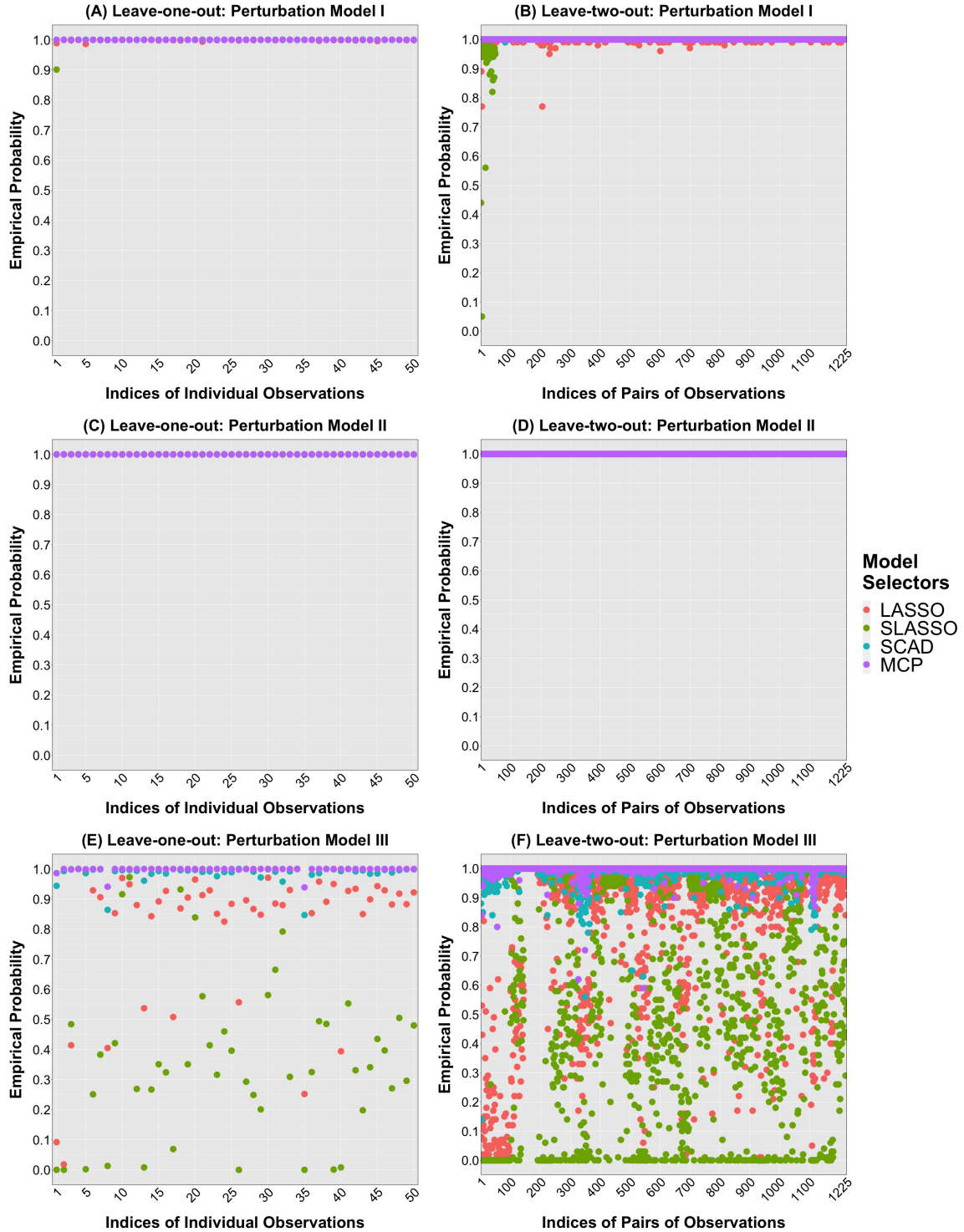


Figure 1: Under  $(n, p) = (50, 100)$ , the empirical probability of selecting an incorrect submodel based on the reduced dataset obtained upon removing one or two observations, where the first five points are set to be influential generated by the Motivating Example Perturbation Models I-III (see Web Appendix A). For panels (A), (C) and (E), the 50 reduced datasets are obtained upon removing each single point out of the 50 observations. For panels (B), (D) and (F), the 1225 reduced datasets are obtained upon removing each two-observation pair out of the  $\binom{50}{2} = 1225$  possible choices.

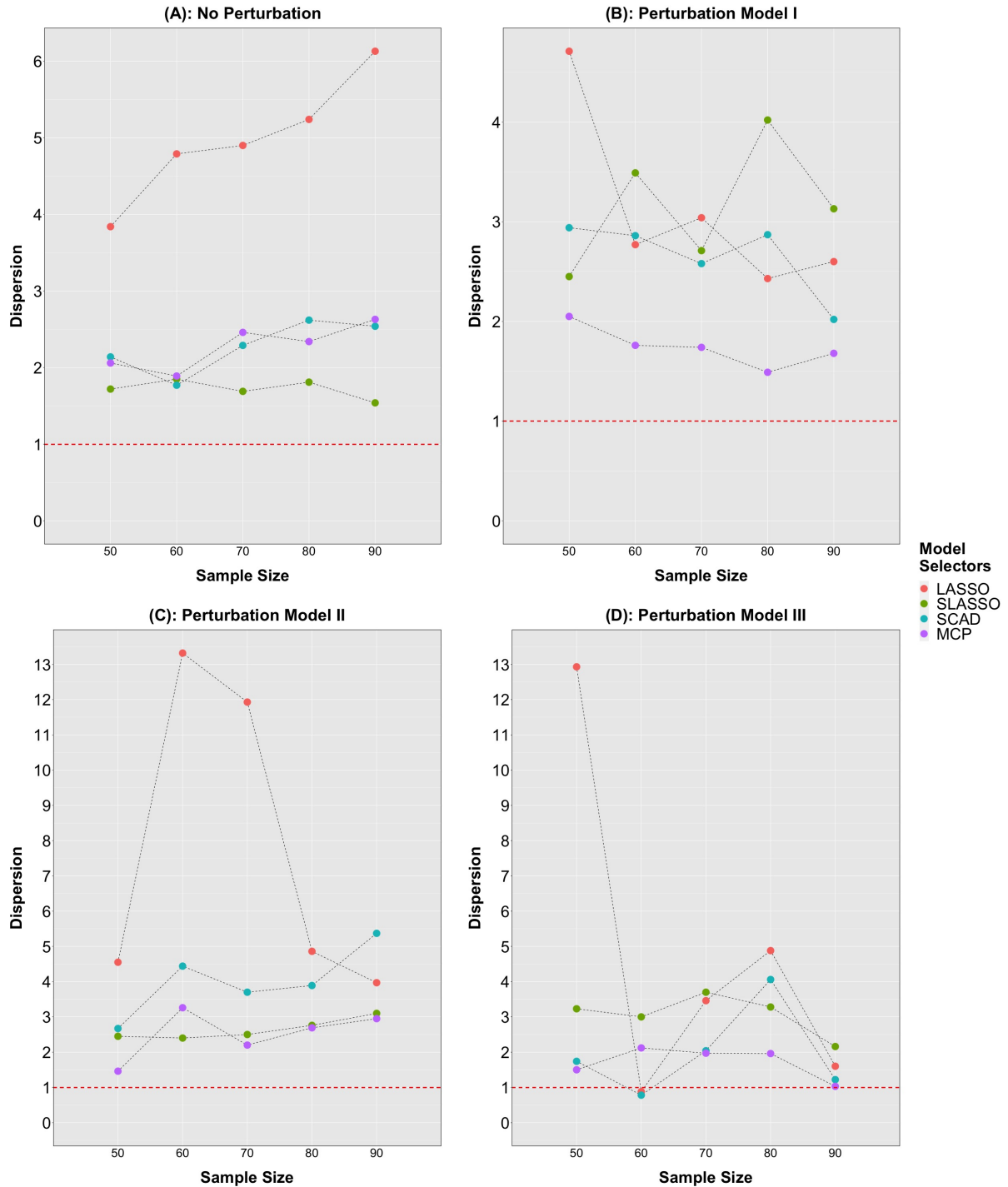


Figure 2: The sample dispersion of  $\tau_{[n]}$ , computed as the quotient of its sample variance divided by the sample mean. The  $\tau_{[n]}$  is generated by different perturbation schemes (Panels (A) to (D)) and model selectors (LASSO, SLASSO, SCAD and MCP) (see Web Appendix G for details). Here, the sample size  $n$  is fixed at 50, 60, 70, 80, 90 and  $p = 2n$ .

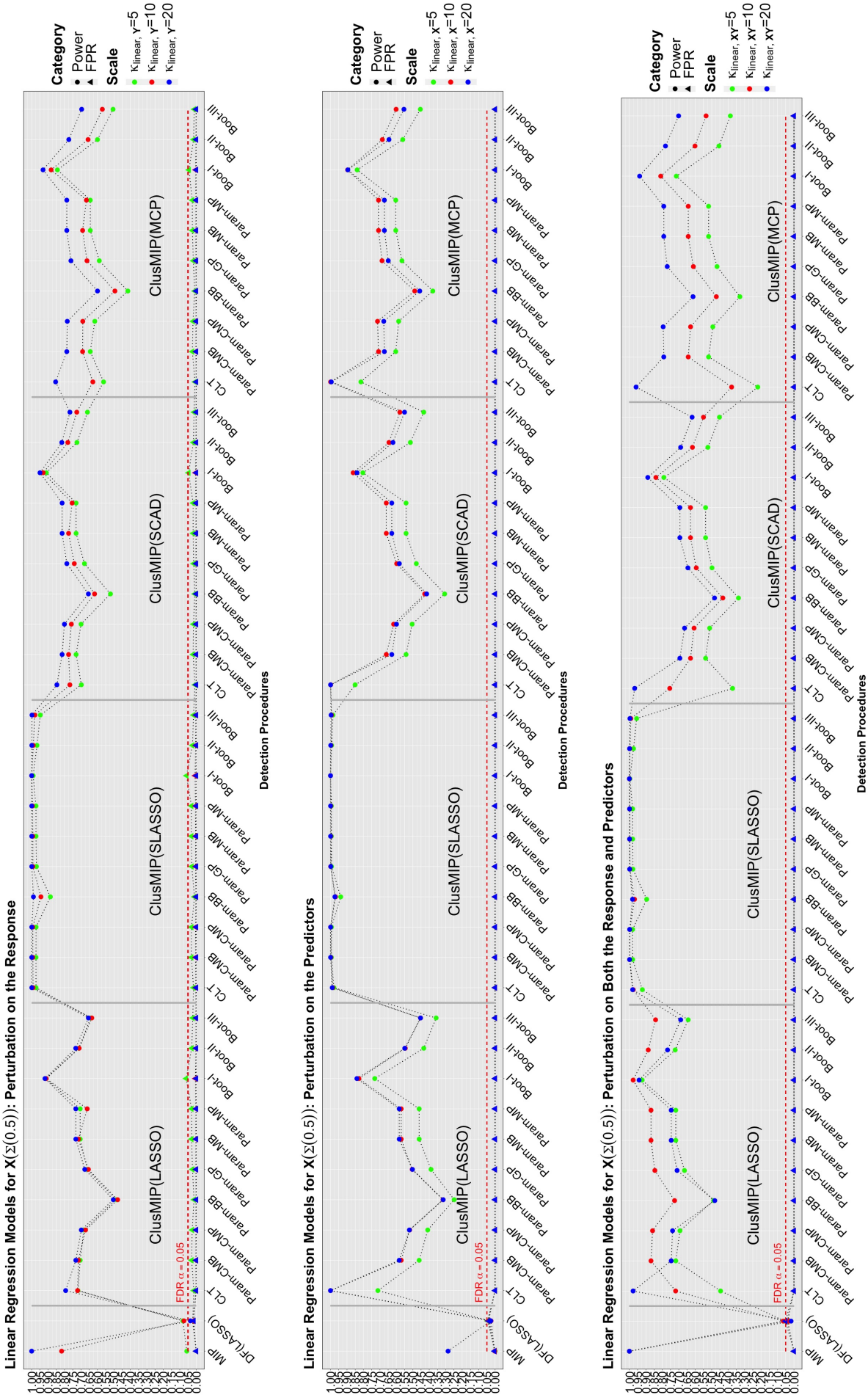


Figure 3: Simulation results (power and FPR) under  $\mathbf{X}(\Sigma(0.5))$  for Perturbation Models I (upper panel), II (middle panel) and III (lower panel).

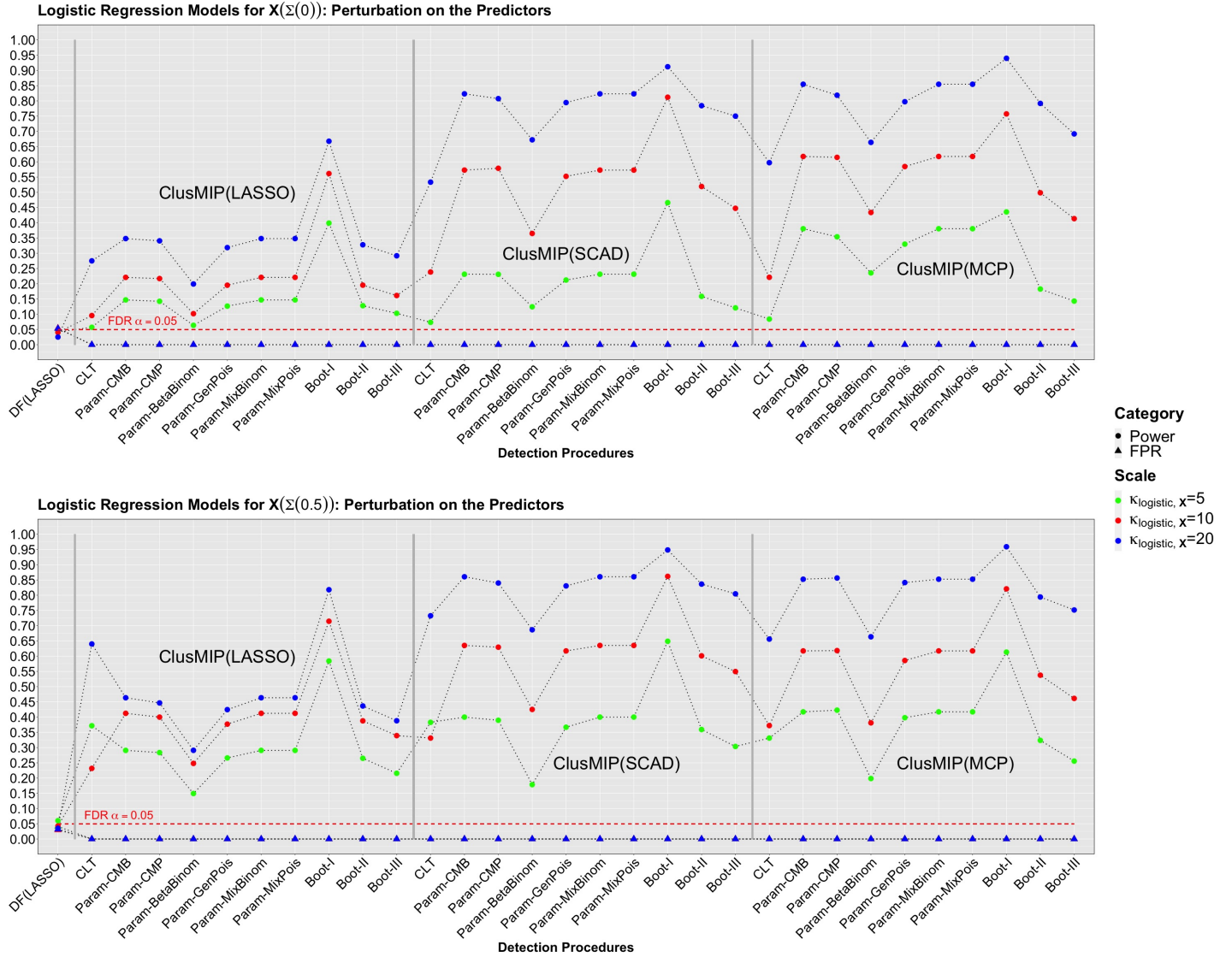


Figure 4: Simulation results (power and FPR) under the logistic regression model (4) for  $\mathbf{X}(\Sigma(0))$  (upper panel) and  $\mathbf{X}(\Sigma(0.5))$  (lower panel).

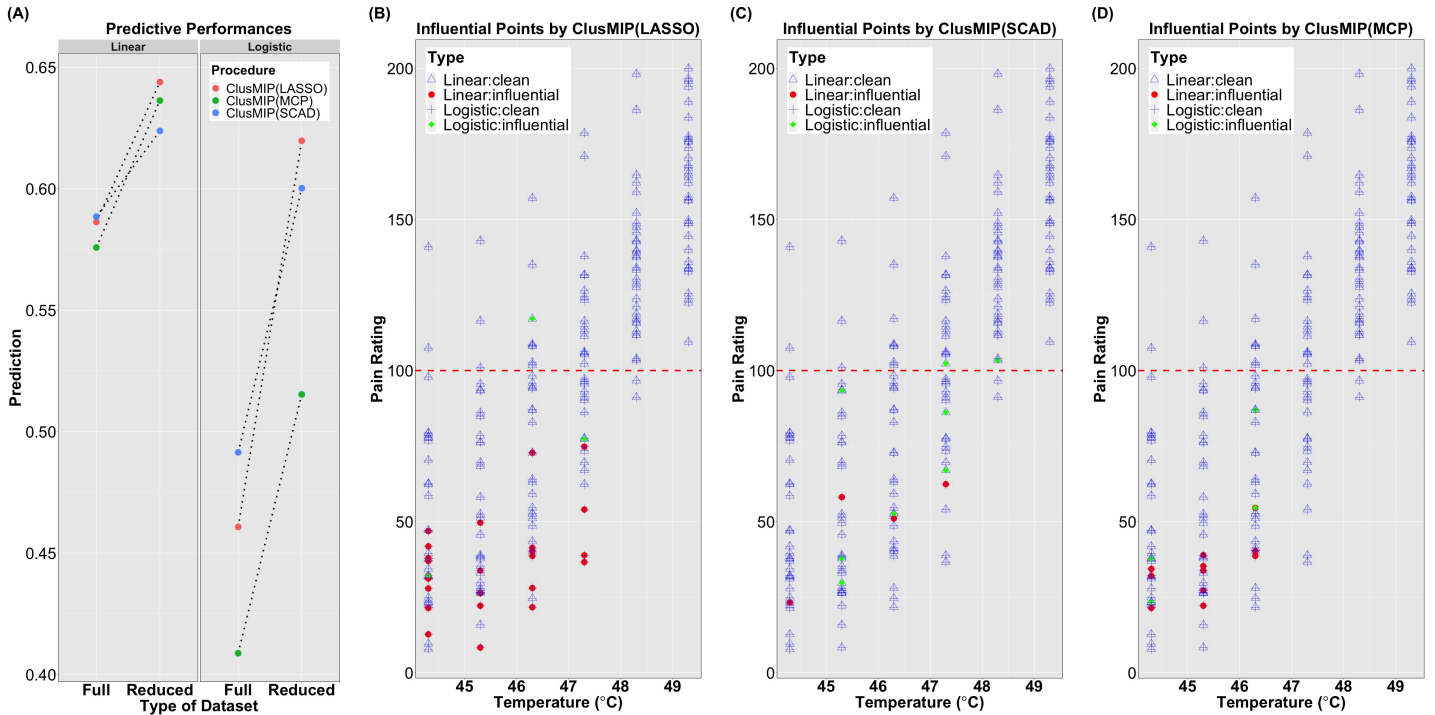


Figure 5: Real data analysis on pain prediction using fMRI data. Panel (A): comparison of predictive performance before and after removing detected influential points under (1) and (4). Panels (B) to (D): for the revised ClusMIP applied to the LASSO, SCAD and MCP, the distribution of detected influential observations and the remaining clean observations under (1) and (4) mapped back to the pain ratings classified according to the six temperatures.



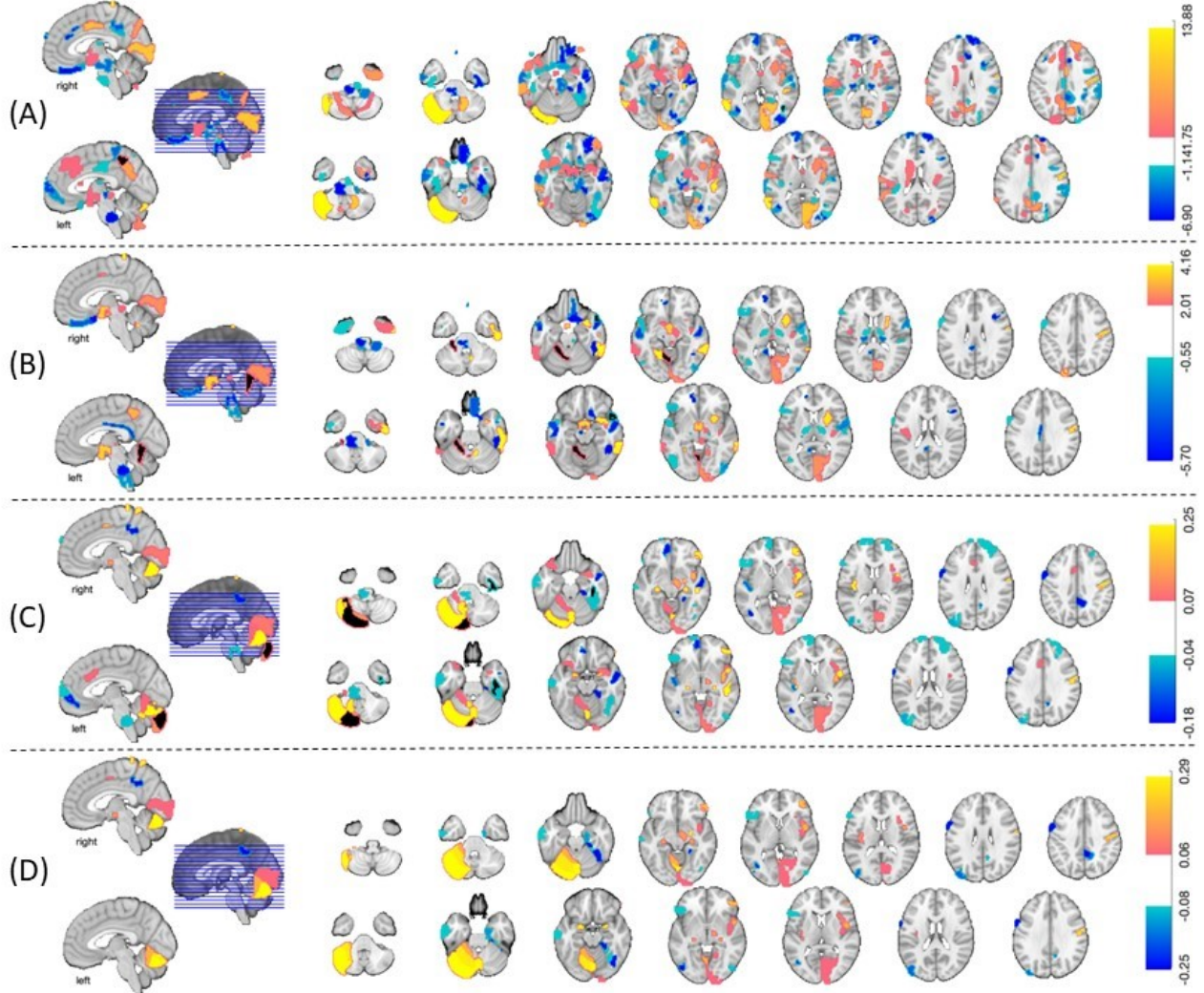


Figure 6: Real data analysis on pain prediction using fMRI data: selection of brain regions and the corresponding magnitude of the LASSO regression coefficients. Panel (A): linear regression model based on the full dataset. Panel (B): linear regression model based on the reduced dataset upon removing influential points given by  $\hat{I}_{\text{linear}}(\text{ClusMIP}(\text{LASSO}))$  with Boot-I. Panel (C): logistic regression model based on the full dataset. Panel (D): logistic regression model based on the reduced dataset upon removing influential points given by  $\hat{I}_{\text{logistic}}(\text{ClusMIP}(\text{LASSO}))$  with Boot-I. Here, Boot-I is the first bootstrap scheme to derive threshold of  $\tau_{[n]}$  for diagnosis purposes discussed in Section 2.4.2.